Quasi-free-standing graphene nano-islands on Ag(110), grown from solid carbon source

Rongting Wu, Junhai Ren, Li Dong, Yeliang Wang, Qing Huan, and H.-J. Gao

Citation: Appl. Phys. Lett. **110**, 213107 (2017);
View online: https://doi.org/10.1063/1.4984093
View Table of Contents: http://aip.scitation.org/toc/apl/110/21
Published by the American Institute of Physics

Quasi-free-standing graphene nano-islands on Ag(110), grown from solid carbon source

Rongting Wu,[1,2,a)] Junhai Ren,[1,2,a)] Li Dong,[1,2] Yeliang Wang,[1,2,3,b)] Qing Huan,[1,2,b)] and H.-J. Gao[1,2,3]
[1]*Institute of Physics and University of Chinese Academy of Sciences, Chinese Academy of Sciences, Beijing 100190, China*
[2]*Beijing Key Laboratory for Nanomaterials and Nanodevices, Beijing 100190, China*
[3]*Collaborative Innovation Center of Quantum Matter, Beijing 100084, China*

(Received 7 April 2017; accepted 12 May 2017; published online 24 May 2017)

Structural, electronic, and mechanical properties of graphene islands grown by depositing carbon atoms directly onto a hot single crystal Ag(110) surface are experimentally investigated. First, graphene nano-islands with morphologies tuned by carbon flux and substrate temperatures are fabricated. Moiré superstructures are found to be superposed on the graphene islands, corresponding to the islands' varied orientations and periodicities with respect to the underlying Ag(110) substrate. Both Scanning tunnelling spectroscopy and Raman spectroscopy indicate a weak interaction between graphene and the substrate, which is further confirmed by scanning tunnelling microscopy tip induced graphene flake movement. *Published by AIP Publishing.*
[http://dx.doi.org/10.1063/1.4984093]

Graphene has aroused extensive interest due to its fascinating physical properties such as quantum electronic transport,[1,2] tunable bandgap,[3] high elasticity,[4] and high quantum efficiency for light–matter interactions[5,6] since its isolation in 2004.[7] Among the various fabrication methods, epitaxial growth on transition metal substrates[8–15] has been reported to yield large scale, single crystal continuous graphene. Nevertheless, the interaction between graphene and general transition metal substrates greatly affects the intrinsic electronic structure of graphene,[10,14,15] leaving the vibrational states of pristine graphene invisible in the Raman spectra.[16]

Compelling evidence has been published for wide applicability of silver, a chemically inert noble metal, as a substrate for the fabrication of other 2D materials, such as silicene[17,18] and borophene,[19,20] as well as in surface-enhanced plasmonic studies.[21] Therefore, graphene on silver is an attractive system for attempts to integrate graphene with other 2D materials, as well as plasmonic property studies. However, due to silver's low melting point and chemical inertness, research into growing graphene on a silver surface has been limited; only few works have been published, employing Ag(111)[22,23] and Ag(001).[24] Compared with these smooth silver surfaces, the Ag(110) surface has parallel atomic channels along the [1 $\bar{1}$ 0] direction with a width of 4 Å, which will certainly induce anisotropy and diversity in the materials on top, e.g., aligned functional organic nanoribbon has been fabricated on this surface recently.[25] In addition, one of the most exciting graphene research frontiers is the fabrication of quasi-free-standing graphene nanoribbons or nano-islands, which are believed to possess peculiar electronic and magnetic properties,[26] such as tunable bandgaps,[3] localized edge stages,[27,28] and spin polarization.[29,30]

Here, we report growth of quasi-free-standing graphene nano-islands by depositing carbon atoms directly onto a hot single-crystal Ag(110) surface. By changing the deposition flux and substrate temperatures, we fabricate graphene nano-islands with different morphologies on a single crystal Ag(110) surface. Atomic-resolved scanning tunnelling microscopy (STM) images reveal that the nano-islands assume different orientations on the substrate, leading to different "strip like" moiré superstructures. With accurately measured relative orientations of graphene and Ag(110) surface, we build geometrical models for the moiré superstructures of graphene on the Ag(110) surface, which show good agreement with the experimental morphology. Scanning tunnelling spectroscopy (STS) spectra taken from graphene nanoflakes clearly reveal intrinsic graphene electronic properties. In addition, vibrational peaks in the Raman spectra are characteristic of pristine graphene, indicating a weak interaction between the graphene nano-islands and the Ag(110) surface, which is further confirmed by a graphene nanoflake being moved by the STM tip during detailed STM measurements.

More specifically, our experiments were carried out in a homemade ultrahigh vacuum (UHV) STM[31] system with base pressure lower than 2×10^{-10} mbar. The single crystal Ag(110) (roughness <30 nm, orientation accuracy <0.1°, MaTeck Company) was prepared in a ultrahigh vacuum by repeated cycles of Ne^+ ion sputtering and subsequent annealing at 770 K until a clean, atomically flat surface was confirmed by STM imaging. A solid carbon source in a rod form was degassed by a sublimation process with a homemade e-beam evaporator in the UHV chamber for 2 h before graphene growth. The carbon atoms were evaporated by using an e-beam evaporator with different fluxes during the experiment, while the substrate Ag(110) was kept at elevated temperature. For the purposes of this paper, monolayer (ML) is defined as the amount of graphene that entirely covers the substrate surface. All the STM images were taken *in-situ* using the constant-current mode at room temperature with

[a)]R. Wu and J. Ren contributed equally to this paper.
[b)]Electronic addresses: ylwang@iphy.ac.cn and huanq@iphy.ac.cn

bias applied to the sample. The STS spectra were taken at low temperature by cooling both the sample and the scanner down to 100 K, using a continuous cooling method. Raman spectra were acquired *ex-situ* by using a Renishaw spectrometer at 532 nm with 1 mW power.

Generally, graphene growth by chemical vapor deposition (CVD) involves two processes: breaking of carbon bonds in the precursor and formation of carbon bonds in the graphene. In particular, in the cases of different transition metals, during graphene growth, they serve not only as the substrate but also as a catalyst for breaking and formation of carbon bonds. Due to silver's inertness and low melting temperature, it is next to impossible to grow graphene on silver surface via normal CVD.

To enable the carbon bonds to break and fresh ones to form, in the present work we employed a pure carbon rod as the precursor, melted the carbon rod using an e-beam evaporator, and then directly spread isolated carbon atoms onto a hot Ag(110) surface. The substrate was kept at around 770 K during the graphene growth. A schematic of the experiment appears in Fig. 1(a). A typical atomic channel along the [1 $\bar{1}$ 0] direction is indicated by the blue arrow. We find that very low carbon flux is critical for graphene growth on Ag(110). Figure 1(b) shows the morphology of a graphene nano-island grown with a carbon flux of 0.57 ML/h, while keeping the substrate at 770 K. Obviously, the graphene nano-island has a dendrite-like structure, with many white clusters localized both in the center and at the growth front of the nano-islands.

To study the influence of the carbon flux on the graphene nano-islands' morphology, we grew graphene with a flux of 0.57 ML/h for 20 min and then switched to 0.09 ML/h for another 20 min; one resulting graphene nano-island is shown in Fig. 1(c). Comparing Fig. 1(b) with Fig. 1(c), we can see that a white cluster exists in the center of each of the graphene nano-islands, and the growth front of the nano-island in Fig. 1(c) is free of white clusters. Therefore, we conclude that the central white cluster serves as the growth seed of the graphene nano-island, and with low carbon flux, the deposited carbon atoms have enough time to move to the nanoflake's edges before too many new carbon atoms land, resulting in a cluster-free growth front, see Fig. 1(c).

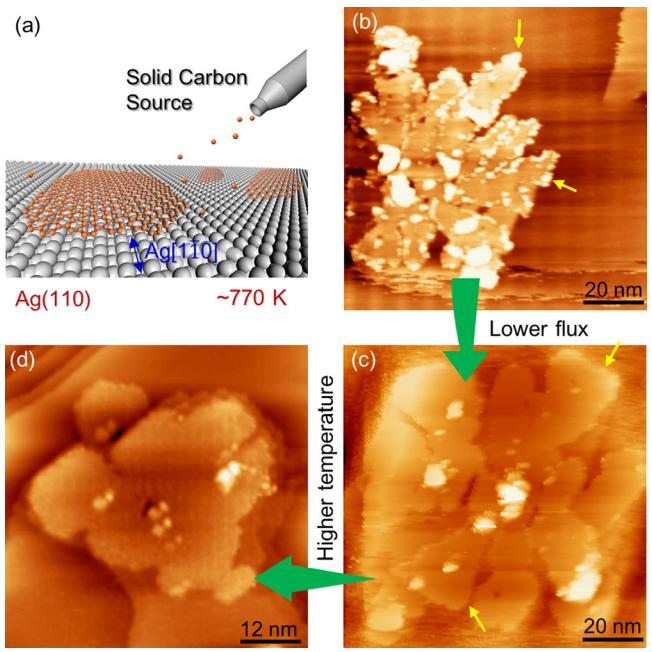

FIG. 1. Experimental schematic and STM images of the graphene nano-island grown in different experimental conditions on Ag(110). (a) Schematic of direct growth of graphene nano-islands on Ag(110). (b) Fractal morphology of the graphene nano-island on Ag(110) fabricated by growing at a rate of 0.57 ML/h, while keeping the substrate at 770 K. (c) Typical morphology of the graphene nano-island fabricated by growing at a rate of 0.57 ML/h for 20 min and then switching to a 0.09 ML/h for another 20 min, with the substrate kept at 770 K. (d) Typical morphology of the graphene nano-island fabricated by growing at a rate of 0.09 ML/h while keeping the substrate at 800 K.

On the other hand, if the carbon flux is too high, newly arrived carbon atoms accumulate with the previously deposited carbon atoms before the latter reach the growth front of the nano-island, so white clusters form on the surface, see Fig. 1(b). Figure 1(d) shows the typical morphology of a graphene nano-island grown at a rate of 0.09ML/h while keeping the substrate at 800 K. Obviously, there are fewer white clusters both in the center and in the growth front. Furthermore, comparing the graphene nano-islands grown in the three different procedures, we see that the shape gradually evolves from the dendrite-like structure to a fairly uniform, smooth-edged structure with decreasing flux and increasing substrate temperature. Therefore, lower carbon flux and higher substrate temperature favor the formation of uniform, smooth-edged graphene nano-islands with fewer white clusters on the surface.

To get a clear understanding of the orientation and structure of the graphene nano-islands on Ag(110), high-resolved STM images were obtained, as shown in Fig. 2. From the atomic-resolution images of the substrate, we identify the [1 $\bar{1}$ 0] direction of the atomic channel on the surface, as indicated by the blue arrow in Fig. 2(a). All the angles exhibited in other images are relative to the [1 $\bar{1}$ 0] direction. Here, we have designated the counterclockwise direction as positive and clockwise as negative. Obviously, the three adjacent graphene nano-islands in Fig. 2(a) have assumed different atomic orientations, depicted by the black arrows, which is the main reason for the gaps between them, highlighted by the white dashed lines.

During the experiment, in addition to elucidating the atomic structure of the graphene nano-islands, we detected some larger modulated structures on the graphene nano-islands, indicated by green and red ovals in Figs. 2(b) and 2(c). These two figures are atomic-resolved STM images which clearly show the details of the relationship between the atomic structure of the graphene lattice and the larger modulations indicated by the green and red ovals. Obviously, for graphene islands with differing orientations, both the size and orientation of the larger pattern of modulation vary a lot. One possible explanation for these larger modulated structures is moiré superstructures arising from the lattice mismatch between the graphene and the underlying Ag(110) substrate. To verify this hypothesis, we constructed a geometrical model by directly superposing the graphene lattice on Ag(110) substrate and tuning the relative orientation between them to the same angle as observed in the experiment, as depicted in Fig. 2(d). Comparing the high-resolution STM image in Fig. 2(c) with the geometrical model in Fig. 2(d), we can see that both the graphene atomic

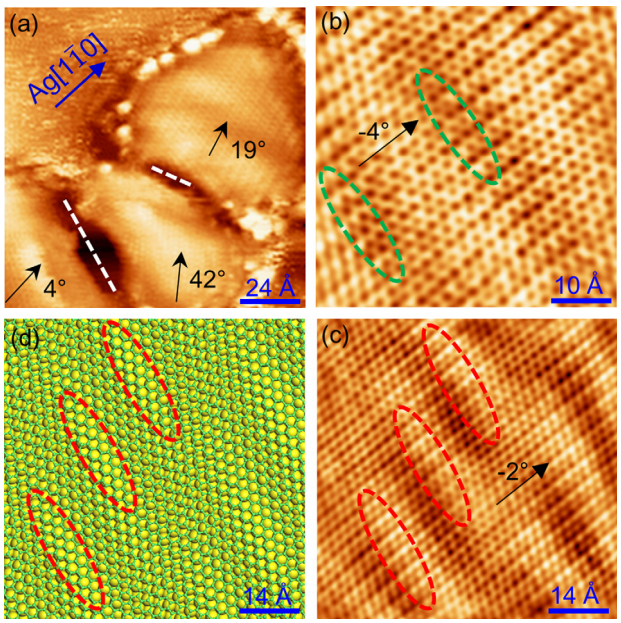

FIG. 2. Different rotation angles and moiré superstructures of graphene nano-islands on Ag(110). (a) Three discontinuous graphene nano-islands on the Ag(110) surface with the arrows indicating the atomic orientations with respect to the [1 $\bar{1}$ 0] direction of the substrate. (b) and (c) at atomic resolution show the moiré superstructures on graphene nano-islands with different rotation angles on Ag(110). (d) Geometric model of graphene on Ag(110) with the same rotation angle as in Fig. 2(c), which produces the same moiré superstructure indicated by the red ellipses.

lattice and the larger modulation structures agree very well in these two pictures, which clearly confirms that these larger modulation structures are moiré superstructures.

By further analysis of the geometric model, one can see that the oval highlighted areas share a common relative position between the atoms from graphene and the underlying substrate. The modulation of the relative position between atoms from the graphene and the underlying substrate introduces corresponding modulation of the electronic density of states (DOS) and then leads to the periodic moiré superstructures detected in the STM characterization. Furthermore, since even slight rotation of the graphene lattice produces a large difference in the moiré superstructures, as shown in Figs. 2(b) and 2(c), the moiré superstructures could be employed as a magnification of graphene rotation. Therefore, from the various moiré superstructures on the graphene nano-islands, we conclude that graphene regions with different orientations are common on the Ag(110) surface. Considering previous work regarding graphene on transition metals, rotation domains usually appear on metals with a weak interaction with the graphene, such as Pt(111)[32] and Ir(111),[33,34] rather than metals with a strong interaction with the graphene, such as Ru(0001).[13] Therefore, we can assume a fairly weak interaction between the graphene and the underlying Ag(110) substrate.

To explore the interaction between graphene nano-islands and the underlying Ag(110) surface, we carried out *in-situ* local STS measurements. Figure 3(a) shows a high-resolution STM image of a graphene nano-island on Ag(110), wherein atomic resolution of both graphene and the Ag(110) substrate has been obtained, with unit cells highlighted by a black diamond and a blue rectangle, respectively.

To get detailed knowledge of the electronic properties of the nano-islands, STS measurements were carried out at five different points along the green dashed line in Fig. 3(a), obtaining the respective STS curves in Fig. 3(b). Comparing spots 1 and 2 on the bare Ag(110) surface, both of their STS curves are fairly flat; however, for the spot closer to the graphene nano-island, the electronic density of states rises in both positive and negative voltage ranges. We attribute these rises in the STS curve to the size effect of the STM tip, which is usually tens of nanometers; thus, the electronic density of states of graphene will be superposed when the spot is too close to a graphene nanoflake. Curve 3, taken on the edge of a graphene nanoflake, shows more enhancement of the electronic density of states in both the positive and negative ranges. When the tip was moved to points 4 and 5 on the graphene nano-island, a clear V-shape appeared, clearly resembling the Dirac cone structure of intrinsic graphene. From the local minimum of the dI/dV curve with the gaplike feature[35–37] around the Fermi energy, the position of the Dirac point is estimated in the range of −20 mV to −45 mV, indicating an electron doping from the underline Ag(110) substrate.

As Raman spectroscopy has been widely used in characterizing the properties of graphene materials, we employed it to characterize the physical properties of these nano-islands. The Raman spectra were acquired *ex-situ* using a Renishaw spectrometer at 532 nm with 1 mW power. Figure 3(c) shows a typical Raman spectrum of graphene nano-islands on Ag(110); the common peaks of graphene, such as D (∼1347.5 cm^{-1}), G (1595.6 cm^{-1}), and 2D (2689 cm^{-1}), can be observed. In addition, the spectrum includes one shoulder at 1624 cm^{-1} and another peak at 2942.7 cm^{-1}, which correspond, respectively, to the defect-related D' peak and the D + G peak.[38,39] The distinct D peak and the appearance of the D' shoulder and D + G peak are usually related to edge defects of single-crystal graphene domains as well as point defects within the basal plane.[40] Here, the I(D)/I(D') ratio is around ∼3.5, which has been linked to a higher concentration of edge defects as opposed to vacancy defects and sp^3 hybridizations in the basal plane.[41] Considering that the laser spot size is larger than 1 μm and most of the graphene nano-islands grown in this work are only tens of nano-meters, it is obvious that the proportion of edge defects is much greater than that would be found in large scale, continuous graphene grown on a transition metal surface.[10,13,32] However, in most graphene directly grown on a transition metal surface, no Raman signal could be detected, so the Raman signal from graphene nano-islands on Ag(110) provides convincing evidence for the weak interaction between the graphene and the underlying Ag(110) surface.

Furthermore, detailed STM examination shows that a graphene nano-island can be moved by the STM tip during the normal scanning process. Figures 3(d) and 3(e) present two successive STM images of the same graphene nano-island with the same scanning parameters of −1.0 V and 0.1 nA, and notably, one flake of the graphene nano-island, highlighted by the blue dashed line, was moved, as revealed by the difference between Figs. 3(d) and 3(e). This kind of tip-induced graphene movement has been reported only on graphite[42] and gold substrates,[43] both of which interact very

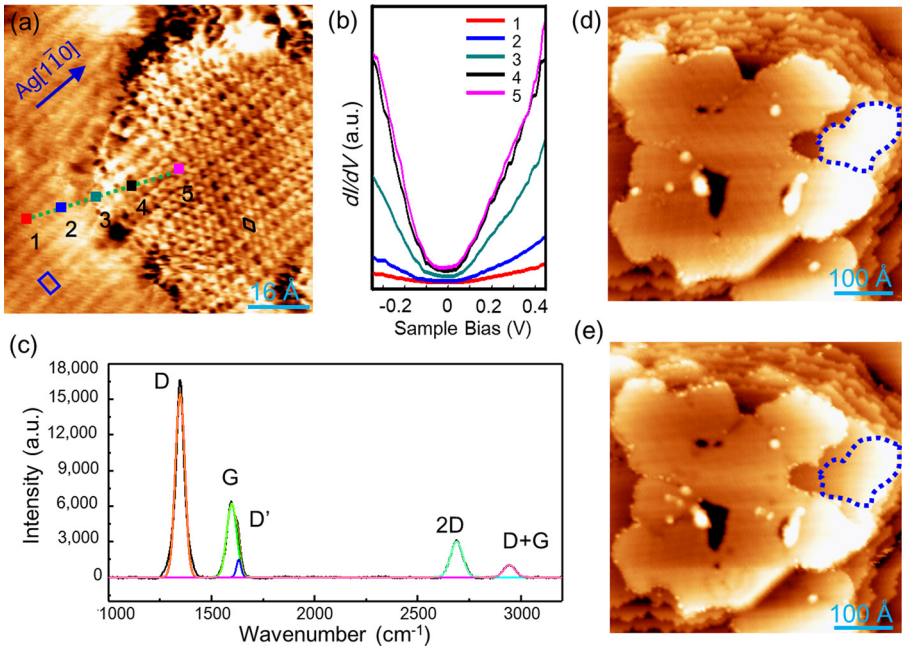

FIG. 3. *In-situ* local scanning tunneling spectroscopy and *ex-situ* macroscopic Raman data of graphene nano-islands on the Ag(110) surface. (a) High resolution STM images of a graphene island on Ag(110), with atomic resolution of both the substrate and graphene. (b) Differential conductance of the five different positions shown in (a). For spots 4 and 5 on the graphene nano-island, the Dirac cone structure is observed, indicating electronic properties of intrinsic graphene. (c) Raman spectrum of graphene nano-islands on the Ag(110) surface; the typical D band, G band, 2D band, and D + G band are clearly resolved, implying the weak interaction between graphene nano-islands and the underlying Ag(110) substrate. (d) and (e) STM images of the same graphene nano-island before and after scanning; one flake of the island, highlighted by the blue dashed line, was inadvertently moved, which further indicates the weak interaction between the islands and the Ag(110) surface; the scanning parameters for (d) and (e) are −1.0 V and 0.1 nA.

weakly with the graphene on top. Therefore, considering *in-situ* local STS spectra, tip manipulation, and macroscopic Raman data together, we conclude that the graphene nano-islands grown on Ag(110) interact very weakly with the substrate and behave like quasi-free-standing graphene.

In summary, we successfully fabricated quasi-free standing graphene nano-islands on the Ag(110) surface with a solid carbon source. By changing the deposition flux and substrate temperature, graphene nano-islands with different morphologies were fabricated. Atomic-resolved STM images reveal that the graphene nanoflakes adopt different orientations on the substrate, leading to different "strip like" moiré superstructures in the graphene. With accurately measured relative angles between graphene and the substrate, we build a geometrical model to simulate the moiré superstructures of the graphene sheet, which shows good agreement with the experimental data. STS spectra taken from the nano-islands clearly reveal intrinsic graphene electronic properties. Observation of the pristine graphene vibrational peaks in the Raman spectra also indicates a very weak interaction between the graphene and the Ag(110) surface. The weak interaction is further confirmed by noting that a nano-flake was moved by the STM tip. Considering the plasma enhancement effect of the silver surface, these quasi-free standing graphene nano-islands on Ag(110) are promising for further studies of graphene plasmonic properties and related graphene optoelectronic phenomena in the future.

Financial support of this work by the National Key Scientific Instrument and Equipment Development Project of China (Nos. 2013YQ12034501 and 2013YQ12034503), National Key Research and Development Projects of China (2016YFA0202300), National Basic Research Program of China (2013CBA01600), the NSFC (Nos. 51572290, 11204361, 61390501, 11334006, and 51325204), and the Chinese Academy of Sciences (Nos. 1731300500015 and XDB07030100) is gratefully acknowledged.

[1]K. S. Novoselov, A. K. Geim, S. V. Morozov, D. Jiang, M. I. Katsnelson, I. V. Grigorieva, S. V. Dubonos, and A. A. Firsov, Nature **438**(7065), 197 (2005).
[2]Y. B. Zhang, Y. W. Tan, H. L. Stormer, and P. Kim, Nature **438**(7065), 201 (2005).
[3]M. Y. Han, B. Özyilmaz, Y. Zhang, and P. Kim, Phys. Rev. Lett. **98**(20), 206805 (2007).
[4]C. Lee, X. D. Wei, J. W. Kysar, and J. Hone, Science **321**(5887), 385 (2008).
[5]A. N. Grigorenko, M. Polini, and K. S. Novoselov, Nat. Photonics **6**(11), 749 (2012).
[6]Y. Liu, R. Cheng, L. Liao, H. Zhou, J. Bai, G. Liu, L. Liu, Y. Huang, and X. Duan, Nat. Commun. **2**, 579 (2011).
[7]K. S. Novoselov, A. K. Geim, S. V. Morozov, D. Jiang, Y. Zhang, S. V. Dubonos, I. V. Grigorieva, and A. A. Firsov, Science **306**(5696), 666 (2004).
[8]Y. S. Dedkov, M. Fonin, U. Ruediger, and C. Laubschat, Phys. Rev. Lett. **100**(10), 107602 (2008).
[9]L. Gao, J. R. Guest, and N. P. Guisinger, Nano Lett. **10**(9), 3512 (2010).
[10]A. T. N'diaye, J. Coraux, T. N. Plasa, C. Busse, and T. Michely, New J. Phys. **10**, 043033 (2008).
[11]Y. Pan, D.-X. Shi, and H.-J. Gao, Chin. Phys. **16**(11), 3151 (2007).
[12]P. W. Sutter, P. M. Albrecht, and E. A. Sutter, Appl. Phys. Lett. **97**(21), 213101 (2010).
[13]Y. Pan, H. Zhang, D. Shi, J. Sun, S. Du, F. Liu, and H-j. Gao, Adv. Mater. **21**(27), 2777 (2009).
[14]M. Batzill, Surf. Sci. Rep. **67**(3–4), 83 (2012).
[15]D. Yuriy and V. Elena, J. Phys.: Condens. Matter **27**(30), 303002 (2015).
[16]E. Starodub, A. Bostwick, L. Moreschini, S. Nie, F. El Gabaly, K. F. Mccarty, and E. Rotenberg, Phys. Rev. B **83**(12), 125428 (2011).
[17]B. J. Feng, Z. J. Ding, S. Meng, Y. G. Yao, X. Y. He, P. Cheng, L. Chen, and K. H. Wu, Nano Lett. **12**(7), 3507 (2012).

[18]B. Lalmi, H. Oughaddou, H. Enriquez, A. Kara, S. Vizzini, B. Ealet, and B. Aufray, Appl. Phys. Lett. **97**(22), 223109 (2010).
[19]A. J. Mannix, X. F. Zhou, B. Kiraly, J. D. Wood, D. Alducin, B. D. Myers, X. L. Liu, B. L. Fisher, U. Santiago, J. R. Guest *et al*., Science **350**(6267), 1513 (2015).
[20]B. J. Feng, J. Zhang, Q. Zhong, W. B. Li, S. Li, H. Li, P. Cheng, S. Meng, L. Chen, and K. H. Wu, Nat. Chem. **8**(6), 563 (2016).
[21]R. Zhang, Y. Zhang, Z. C. Dong, S. Jiang, C. Zhang, L. G. Chen, L. Zhang, Y. Liao, J. Aizpurua, Y. Luo *et al*., Nature **498**(7452), 82 (2013).
[22]B. Kiraly, E. V. Iski, A. J. Mannix, B. L. Fisher, M. C. Hersam, and N. P. Guisinger, Nat. Commun. **4**, 2804 (2013).
[23]J. Tesch, P. Leicht, F. Blumenschein, L. Gragnaniello, M. Fonin, L. E. Marsoner Steinkasserer, B. Paulus, E. Voloshina, and Y. Dedkov, Sci. Rep. **6**, 23439 (2016).
[24]S. Grandthyll, K. Jacobs, and F. Muller, Phys. Status Solidi B **252**(8), 1695 (2015).
[25]N. Kalashnyk, K. Mouhat, J. Oh, J. Jung, Y. Xie, E. Salomon, T. Angot, F. Dumur, D. Gigmes, and S. Clair, Nat. Commun. **8**, 14735 (2017).
[26]D. C. Yu, E. M. Lupton, H. J. Gao, C. Zhang, and F. Liu, Nano Res. **1**(6), 497 (2008).
[27]Y. Kobayashi, K. Fukui, T. Enoki, and K. Kusakabe, Phys. Rev. B **73**(12), 125415 (2006).
[28]M. Fujita, K. Wakabayashi, K. Nakada, and K. Kusakabe, J. Phys. Soc. Jpn. **65**(7), 1920 (1996).
[29]O. V. Yazyev, Rep. Prog. Phys. **73**(5), 056501 (2010).
[30]W. L. Wang, S. Meng, and E. Kaxiras, Nano Lett. **8**(1), 241 (2008).
[31]B. C. Stipe, M. A. Rezaei, and W. Ho, Rev. Sci. Instrum. **70**(1), 137 (1999).
[32]M. Gao, Y. Pan, L. Huang, H. Hu, L. Z. Zhang, H. M. Guo, S. X. Du, and H. J. Gao, Appl. Phys. Lett. **98**(3), 3 (2011).
[33]E. Loginova, S. Nie, K. Thurmer, N. C. Bartelt, and K. F. Mccarty, Phys. Rev. B **80**(8), 085430 (2009).
[34]L. Meng, R. T. Wu, L. Z. Zhang, L. F. Li, S. X. Du, Y. L. Wang, and H. J. Gao, J. Phys.-Condens. Matter **24**(31), 314214 (2012).
[35]Y. Zhang, V. W. Brar, F. Wang, C. Girit, Y. Yayon, M. Panlasigui, A. Zettl, and M. F. Crommie, Nat. Phys. **4**(8), 627 (2008).
[36]L. Meng, R. T. Wu, H. T. Zhou, G. Li, Y. Zhang, L. F. Li, Y. L. Wang, and H. J. Gao, Appl. Phys. Lett. **100**(8), 4 (2012).
[37]J. H. Mao, L. Huang, Y. Pan, M. Gao, J. F. He, H. T. Zhou, H. M. Guo, Y. Tian, Q. Zou, L. Z. Zhang *et al*., Appl. Phys. Lett. **100**(9), 093101 (2012).
[38]L. M. Malard, M. A. Pimenta, G. Dresselhaus, and M. S. Dresselhaus, Phys. Rep.-Rev. Sect. Phys. Lett. **473**(5–6), 51 (2009).
[39]D. Bischoff, J. Guettinger, S. Droescher, T. Ihn, K. Ensslin, and C. Stampfer, J. Appl. Phys. **109**(7), 073710 (2011).
[40]A. C. Ferrari, Solid State Commun. **143**(1–2), 47 (2007).
[41]A. Eckmann, A. Felten, A. Mishchenko, L. Britnell, R. Krupke, K. S. Novoselov, and C. Casiraghi, Nano Lett. **12**(8), 3925 (2012).
[42]Y. Gan, W. Chu, and L. Qiao, Surf. Sci. **539**(1–3), 120 (2003).
[43]P. Leicht, L. Zielke, S. Bouvron, R. Moroni, E. Voloshina, L. Hammerschmidt, Y. S. Dedkov, and M. Fonin, ACS Nano **8**(4), 3735 (2014).